

First-Principles Approach to Electrorotation Assay

J. P. Huang and K. W. Yu

Department of Physics, The Chinese University of Hong Kong, Shatin, NT, Hong Kong

Abstract

We have presented a theoretical study of electrorotation assay based on the spectral representation theory. We consider unshelled and shelled spheroidal particles as an extension to spherical ones. From the theoretical analysis, we find that the coating can change the characteristic frequency at which the maximum rotational angular velocity occurs. The shift in the characteristic frequency is attributed to a change in the dielectric properties of the bead-coating complex with respect to those of the uncoated particles. By adjusting the dielectric properties and the thickness of the coating, it is possible to obtain good agreement between our theoretical predictions and the assay data.

PACS Number(s): 82.70.-y, 87.22.Bt, 77.22.Gm, 77.84.Nh

arXiv:cond-mat/0107192v1 [cond-mat.soft] 10 Jul 2001

I. INTRODUCTION

When a suspension of colloidal particles or biological cells is exposed to an external electric field, the analysis of the frequency-dependent response yields valuable information on various processes, like the structural (Maxwell-Wagner) polarization effects [1,2]. The polarization is characterized by a variety of the characteristic frequency-dependent changes. While the polarization of biological cells can be investigated by the method of dielectric spectroscopy [3], conventional dielectrophoresis and electrorotation (ER) analyze the frequency dependence of translations and rotations of single cells in an inhomogeneous and rotating external field, respectively [4,5]. With the recent advent of experimental techniques such as automated video analysis [6] as well as light scattering methods [2], the cell movements can be accurately monitored. In ER, the rotating field induces a cell dipole moment which rotates at the angular frequency of the external field. Any dispersion process causes a spatial phase shift between the induced dipole moment and the external field vector, giving rise to a torque which causes rotation of individual cells.

The electrorotation assay is a technique which uses the phenomenon of electrorotation in combination with antibody technology to enable the rapid and accurate detection of analytes in aqueous solutions. In the assay, an analyte is bound to a known particle causing a change in the dielectric properties of the analyte-bead complex over the properties of just the bead. This change in the dielectric properties is subsequently detected using the electrorotation technique described above. Selectivity can be controlled by the choice of binding agents used on the known particle. This assay method can be used with different analytes ranging from whole cells to molecular species.

In this work, we propose the use of the spectral representation [7] for analyzing the electrorotation of particles in suspensions. The spectral representation is a rigorous mathematical formalism of the effective dielectric constant of a two-phase composite material [7]. It offers the advantage of the separation of material parameters (namely the dielectric constant and conductivity) from the cell structure information, thus simplifying the study.

From the spectral representation, one can readily derive the dielectric dispersion spectrum, with the dispersion strength as well as the characteristic frequency being explicitly expressed in terms of the structure parameters and the materials parameters of the cell suspension (see section II.B below). The actual shape of the real and imaginary parts of the permittivity over the relaxation region can be uniquely determined by the Debye relaxation spectrum, parametrized by the characteristic frequencies and the dispersion strengths. So, we can study the impact of these parameters on the dispersion spectrum directly. The same formalism has been used recently to study the dielectric behavior of cell suspensions [8].

II. FORMALISM

We regard a suspension as a composite system consisting of spherical or spheroidal particles of complex dielectric constant $\tilde{\epsilon}_1$ dispersed in a host medium of $\tilde{\epsilon}_2$. A uniform electric field $\mathbf{E}_0 = E_0 \hat{\mathbf{z}}$ is applied to the composites along the z -axis. We briefly review the spectral representation theory of the effective dielectric constant to establish notations.

A. Spectral representation

The spectral representation is a mathematical transformation of the complex effective dielectric constant $\tilde{\epsilon}_e$. In its original form [7], a two-phase composite material is considered, in which inclusions of complex dielectric constant $\tilde{\epsilon}_1$ and volume fraction p are randomly embedded in a host medium of $\tilde{\epsilon}_2$. The complex effective dielectric constant $\tilde{\epsilon}_e$ will in general depend on the constituent dielectric constants, the volume fraction of inclusions as well as the detailed microstructure of the composite materials.

The essence of the spectral representation is to define the following transformations. If we denote a complex material parameter

$$\tilde{s} = \left(1 - \frac{\tilde{\epsilon}_1}{\tilde{\epsilon}_2}\right)^{-1}, \quad (1)$$

then the reduced effective dielectric constant

$$w(\tilde{s}) = 1 - \frac{\tilde{\epsilon}_e}{\tilde{\epsilon}_2}, \quad (2)$$

can be written as

$$w(\tilde{s}) = \sum_n \frac{F_n}{\tilde{s} - s_n}, \quad (3)$$

where F_n and s_n depend only on the microstructure of the composite materials [7]. In Eq.(3), $0 \leq s_n < 1$ is a real number, while F_n satisfies a sum rule [7]:

$$\sum_n F_n = p, \quad (4)$$

where p is the volume fraction of the suspended cells.

As a result, the spectral representation is a useful theory which helps separate the material property from the geometric information. In what follows, we illustrate the spectral representation by the capacitance of simple geometry. In particular, a parallel-plate capacitor is considered as an example. We will discuss two cases, namely, the series combination and the parallel combination.

In the first case, if one inserts a dielectric slab of dielectric constant $\tilde{\epsilon}_1$ and thickness h_1 , as well as a dielectric of $\tilde{\epsilon}_2$ and thickness h_2 (both of the same area A), into a parallel-plate capacitor of total thickness $h = h_1 + h_2$, the overall capacitance C is given by

$$C^{-1} = C_1^{-1} + C_2^{-1}$$

where $C_1 = \tilde{\epsilon}_1 A/h_1$, and $C_2 = \tilde{\epsilon}_2 A/h_2$, A being the area of a plate. On the other hand, we may define the equivalent capacitance as $C = \tilde{\epsilon}_e A/h$, where $\tilde{\epsilon}_e$ is the effective dielectric constant. That is, we replace the composite dielectric by a homogeneous dielectric of dielectric constant $\tilde{\epsilon}_e$.

Let $\tilde{\epsilon}_1 = \tilde{\epsilon}_2(1 - 1/\tilde{s})$, we can express C in the spectral representation,

$$C = \frac{A\tilde{\epsilon}_2}{h} - \frac{A\tilde{\epsilon}_2 h_1/h^2}{\tilde{s} - h_2/h}.$$

In accord with the spectral representation, one may introduce $w(\tilde{s}) = 1 - \tilde{\epsilon}_e/\tilde{\epsilon}_2$, which is in fact the same as $w(\tilde{s}) = 1 - C/C_0$, where C_0 is the capacitance when the plates are all filled

with a dielectric material of $\tilde{\epsilon}_2$, namely, $C_0 = \tilde{\epsilon}_2 A/h$. Thus we obtain

$$w(\tilde{s}) = \frac{h_1/h}{s - h_2/h}.$$

from which we find that the material parameter is separated from the geometric parameter.

The comparison of $w(\tilde{s})$ with Eq.(3) yields

$$F_1 = h_1/h, \quad s_1 = h_2/h.$$

We should remark that F_1 obtained herein is just equal to the volume fraction of the dielectric of $\tilde{\epsilon}_1$, and that s_1 satisfies $0 \leq s_1 < 1$, as required by the spectral representation theory.

Next we consider the parallel combination. If one inserts a material of dielectric constant $\tilde{\epsilon}_1$ and area w_1 as well as a dielectric of $\tilde{\epsilon}_2$ and area w_2 (both of the same thickness h), into a parallel-plate capacitor of total area $A = w_1 + w_2$, the overall capacitance C is given by

$$C = C_1 + C_2$$

where $C_1 = \tilde{\epsilon}_1 w_1/h$, and $\tilde{\epsilon}_2 = \tilde{\epsilon}_2 w_2/h$. Similarly, after introducing the effective dielectric constant $\tilde{\epsilon}_e$, we may define the overall capacitance as $C = \tilde{\epsilon}_e A/h$.

Again, in the spectral representation, let $\tilde{\epsilon}_1 = \tilde{\epsilon}_2(1 - 1/\tilde{s})$, then

$$C = \frac{\tilde{\epsilon}_2 A}{h} - \frac{\tilde{\epsilon}_2 w_1}{h\tilde{s}}.$$

Writing $w(\tilde{s}) = 1 - C/C_0$, we obtain

$$w(\tilde{s}) = \frac{w_1/A}{\tilde{s}}.$$

From this equation, the material parameter is also found to be separated from the geometric parameter. It is clear that $F_1 = w_1/A$, i.e., the volume fraction of the dielectric of $\tilde{\epsilon}_1$, and $s_1 = 0$.

B. Shell-spheroidal model

For inclusions of arbitrary shape, the spectral representation can only be solved numerically [7]. However, analytic solutions can be obtained for isolated spherical and ellipsoidal

particles. For dilute suspensions of prolate spheroidal particles, the particles can be regarded as noninteracting. The problem is simplified to the calculation of s_n with a single particle, which can be solved exactly.

In fact, the suspension of shell-spheroidal particles dispersed in a host medium is a three-component system. Although the spectral representation is generally valid for two-component composites, we have recently shown that it also applies to composites of coated spheres randomly embedded in a host medium [9]. Similarly, we will show that the spectral representation also applies to the suspension of spheroidal particles of complex dielectric constant $\tilde{\epsilon}_1$ coated with a shell of $\tilde{\epsilon}_s$ dispersed in a host medium of $\tilde{\epsilon}_2$, where

$$\tilde{\epsilon} = \epsilon + \sigma/i2\pi f \quad (5)$$

where f is the frequency of the applied field. In what follows, we will show that from the spectral representation, one can obtain the analytic expressions for the characteristic frequency at which the maximum electrorotation velocity occurs. The depolarization factors of the spheroidal particles will be described by a sum rule

$$L_z + 2L_{xy} = 1 \quad (6)$$

where $0 < L_z \leq 1/3$ and L_{xy} are the depolarization factors along the z - and x - (or y -) axes of the spheroidal particle, respectively. In fact, $L_z = L_{xy} = 1/3$ just indicates a spherical particle.

The phenomenon of electrorotation is based on the interaction between a time-varying electric field \mathbf{E} and the induced dipole moment \mathbf{M} . The dipole moment of the particle arises from the induced charges that accumulate at the interface of the particle. The angle between \mathbf{M} and \mathbf{E} is denoted by θ , where $\theta = \omega t$ and $\omega = 2\pi f$ is angular velocity of the rotating electric field. The torque acting on the particle is given by the vector cross product between the electric field and the dipole moment, so that only the imaginary part of the dipole moment contributes to the electrorotation response. In the steady state, the frequency-dependent rotation speed $\Omega(f)$, which results from the balance between the torque and the viscous drag, is given by

$$\begin{aligned}
\Omega(f) &= -F(\epsilon_2, E, \eta) \text{Im}(\tilde{b}_z \langle \cos^2 \theta \rangle + \tilde{b}_{xy} \langle \sin^2 \theta \rangle), \\
&= -F(\epsilon_2, E, \eta) \text{Im}(\tilde{b}_z/2 + \tilde{b}_{xy}/2),
\end{aligned} \tag{7}$$

where E is the strength of the applied electric field and F is a coefficient which is inversely proportional to the dynamic viscosity η of the host medium. For spherical cells, $F = -\epsilon_2 E^2 / 2\eta$. In Eq.(7), $\text{Im}(\dots)$ indicates the imaginary parts of (\dots) , and the angular brackets denote a time average. Since the angular velocity of the rotating field is much greater than the electrorotation angular velocity, i.e., $\omega \gg \Omega$, the time averages are just equal to $1/2$. For a single coated spheroidal particle, the dipole factor \tilde{b}_z is given by [10]

$$\tilde{b}_z = \frac{1}{3} \frac{(\tilde{\epsilon}_s - \tilde{\epsilon}_2)[\tilde{\epsilon}_s + L_z(\tilde{\epsilon}_1 - \tilde{\epsilon}_s)] + (\tilde{\epsilon}_1 - \tilde{\epsilon}_s)y[\tilde{\epsilon}_s + L_z(\tilde{\epsilon}_2 - \tilde{\epsilon}_s)]}{(\tilde{\epsilon}_s - \tilde{\epsilon}_1)(\tilde{\epsilon}_2 - \tilde{\epsilon}_s)yL_z(1 - L_z) + [\tilde{\epsilon}_s + (\tilde{\epsilon}_1 - \tilde{\epsilon}_s)L_z][\tilde{\epsilon}_2 + (\tilde{\epsilon}_s - \tilde{\epsilon}_2)L_z]} \tag{8}$$

where y is the volume ratio of the core to the whole coated spheroid, while b_{xy} can be obtained by replacing L_z with L_{xy} in Eq.(8).

We are now in a position to represent b_z and b_{xy} in the spectral representation. Let $\tilde{\epsilon}_1 = \tilde{\epsilon}_2(1 - 1/\tilde{s})$, and assume $x = \tilde{\epsilon}_s/\tilde{\epsilon}_2$, we obtain

$$\tilde{b}_z = N.P. + \frac{F_1}{\tilde{s} - s_1} \tag{9}$$

where $N.P.$ denotes the nonresonant part [9] which vanishes in the limit of unshelled spheroidal cells. In Eq.(9), the various quantities are given by

$$s_1 = -\frac{\beta}{\gamma}, \tag{10}$$

$$F_1 = \frac{-x^2 y}{\alpha \gamma}, \tag{11}$$

$$N.P. = \frac{-L_z + L_z y + x(-1 + 2L_z + y - 2L_z y) + x^2(1 - L_z - y + L_z y)}{\alpha} \tag{12}$$

$$\alpha = 3L_z - 3L_z^2 - 3L_z y + 3L_z^2 y + x(3 - 6L_z + 6L_z^2 + 6L_z y - 6L_z^2 y)$$

$$x^2(3L_z - 3L_z^2 - 3L_z y + 3L_z^2 y)$$

$$\beta = -L_z + L_z^2 + L_z y - L_z^2 y + x(-L_z^2 - L_z y + L_z^2 y)$$

$$\gamma = L_z - L_z^2 - L_z y + L_z^2 y + x(1 - 2L_z + 2L_z^2 + 2L_z y - 2L_z^2 y)$$

$$+x^2(L_z - L_z^2 - L_z y + L_z^2 y)$$

Note that we have assumed x to be a real number, which will be justified below. After substituting $\tilde{\epsilon} = \epsilon + \sigma/i2\pi f$ into Eq.[9], we rewrite \tilde{b}_z after simple manipulations

$$\tilde{b}_z = (N.P. + \frac{F_1}{s - s_1}) + \frac{\delta\epsilon_1}{1 + if/f_{c1}} \quad (13)$$

with $s = (1 - \epsilon_1/\epsilon_2)^{-1}$ and $t = (1 - \sigma_1/\sigma_2)^{-1}$, where

$$\begin{aligned} \delta\epsilon_1 &= F_1 \frac{s - t}{(t - s_1)(s - s_1)}, \\ f_{c1} &= \frac{1}{2\pi} \frac{\sigma_2 s(t - s_1)}{\epsilon_2 t(s - s_1)}. \end{aligned}$$

Similarly, we may rewrite \tilde{b}_{xy} as

$$\tilde{b}_{xy} = (N.P.' + \frac{F_2}{s - s_2}) + \frac{\delta\epsilon_2}{1 + if/f_{c2}}. \quad (14)$$

Therefore, we obtain

$$\begin{aligned} \delta\epsilon_2 &= F_2 \frac{s - t}{(t - s_2)(s - s_2)}, \\ f_{c2} &= \frac{1}{2\pi} \frac{\sigma_2 s(t - s_2)}{\epsilon_2 t(s - s_2)}. \end{aligned}$$

Note that $N.P.'$, s_2 and F_2 are obtained by replacing L_z with L_{xy} in the expressions for $N.P.$, s_1 and F_1 , respectively.

We have thus predicted that two characteristic frequencies may appear for uncoated or coated spheroidal particles. Previous theories were often limited to spherical particles, i.e., $L_z = L_{xy} = 1/3$. Therefore, only one characteristic frequency exists. We should remark that even though two characteristic frequencies are predicted, only one of them is dominant (see below).

III. NUMERICAL CALCULATIONS

The model put forward in the previous section applies to various situations such as biological cells and polystyrene beads, etc. Here we perform numerical calculations to investigate the characteristic frequency. Let $s = 1.1$, $t = -0.005$, and $\epsilon_2 = 80\epsilon_0$, where ϵ_0 is the

dielectric constant of the vacuum. In Fig.1, we investigate the effect of particle shape on s_1 and f_{c1} (upper panels), and s_1 and f_{c1} (lower panels), for $z = 2$ and $\sigma_2 = 2.9 \times 10^{-5} Sm^{-1}$, where $z = 1/y$, and $z^{1/3} > 1$ reflects the thickness of the shell (or coating). As is evident from the figure, an increase in the dielectric constant ratio x leads to a red-shift of the characteristic frequency. For a certain x , a small depolarization factor, i.e., the particle is largely deviated from spherical shape, may yield a red-shift too.

In Fig.2, we investigate the effect of the depolarization factor on the quantities $-Im[b_z]/2$ and $-Im[b_z/2 + b_{xy}/2]$. It is evident that the effect of b_{xy} on the peak is small as L_z is small, whereas it gives a large effect as L_z is large. Generally speaking, the dipole moment along the x-(or y-) axis strongly affects both the location and the magnitude of the peak of rotation speed. For spheroidal particles, only one peak is found, and the other peak predicted by the theory may be too small to observe.

To our knowledge, there are no experimental data for electrorotation of spheroidal particles. In order to validate our theory, here we considered the spherical particles as a limiting case of our model. In Fig.3, s_1 and f_c are plotted versus x for a spherical bead ($L_z = 1/3$), for different z as $\sigma_2 = 2.9 \times 10^{-5} Sm^{-1}$. For large x , the shell thickness has only a minor effect on the characteristic frequency. Moreover, a thick shell leads to a red shift (blue shift) of the characteristic frequency appear as $x > 1$ ($x < 1$). Also, all the f_c predicted by different z are smaller (larger) than that predicted one at $z = 1$ (i.e., uncoated bead) for $x > 1$ ($x < 1$).

At $x = 1$, i.e., the shell has the same dielectric constant as the host, all the characteristic frequencies predicted by different thickness of shell are the same. Similar conclusions can be obtained not only for spherical shape, but also for prolate spheroidal shape (not shown here).

We attempt to fit our theoretical predictions with experimental data, which are extracted from an assay [11]. In this assay, there cases were studied, all dealing with spherical particles: that is, uncoated beads, beads coated with an antibody with specificity for Giardia (Shell 1), and beads coated with an antibody with specificity for Cryptosporidium (Shell 2). Let $\sigma_2 = 2.18 \times 10^{-5} Sm^{-1}$, $z = 6$, $x = 7.06$ (Shell 1) and 4.63 (Shell 2), and $F = 0.353$ (Without shell),

1.629 (Shell 1) and 2.278(Shell 2). Good agreement between our theoretical predictions and the assay data is shown in Fig.4. From our theory, it is easy to find the corresponding characteristic frequencies at which maximum rotational angular velocity occurs, $f_c = 4.755 \times 10^5 Hz$ (Without shell), $10^5 Hz$ (Shell 1) and $1.415 \times 10^5 Hz$ (Shell 2). From this, we find that the coating leads to a red shift of the characteristic frequency. It is because the dielectric properties of the bead-coating complex have been changed.

We used $x > 1$ in our fitting, i.e., $x = 7.06$ and 4.63 for bead coated with an antibody with specificity for Giardia and Cryptosporidium, respectively. It is known that, for biological cells, such as Giardia and Cryptosporidium, they have structures such as the cell wall, plasma membrane and the cytoplasm, among which the cell wall has a larger conductivity than the suspending medium. Hence, we may safely take $x > 1$.

IV. DISCUSSION AND CONCLUSION

Here we would like to add some comments. We developed simple equations to describe the electrorotation of particles in a suspension from the spectral representation. These equations serve as a basis which describe the parameter dependence of the polarization and thereby enhances the applicability of various cell models for the analysis of the polarization mechanisms. In this connection, the shell-spheroidal cell model may readily be extended to multi-shell cell model. However, we believe that the multi-shell nature of the cell may have a minor effect on the electrorotation spectrum.

We have considered the isolated cell case, which is a valid assumption for low concentration of cells. However, for a higher concentration of cells, we should consider the mutual interaction between cells. For a randomly dispersed cells suspension, we may replace the dielectric constant of the host medium by the effective dielectric constant of the whole suspension.

When a strong rotating electric field is applied to a suspension, the induced dipole moment will induce an overall attractive force between the polarized cells, leading to rapid

the formation of sheet-like structures in the plane of the rotating field. In reality there is a phase shift between the induced dipole moment of the structure and the applied field, and this can lead to electrorotation. However, the situation will be much more difficult than the single-cell case that we have studied because the many-body as well as multipolar interactions between the particles will produce a complicated electrorotation spectrum. Fortunately, our recently developed integral equation formalism [12] can definitely help to solve for the Maxwell-Wagner relaxation spectrum.

In summary, we have presented a theoretical study of electrorotation assay based on the spectral representation theory. We consider unshelled and shelled spheroidal particles as an extension to spherical ones. From the theoretical analysis, we find that the coating can change the characteristic frequency at which maximum rotational angular velocity occurs. By adjusting the dielectric properties and the thickness of the coating, it is possible to obtain good agreement between our theoretical predictions and the assay data.

ACKNOWLEDGMENTS

This work was supported by the Research Grants Council of the Hong Kong SAR Government under grant CUHK 4245/01P. J. P. H. is grateful to Dr. L. Gao and Dr. C. Xu for fruitful discussion. K. W. Y. acknowledges the hospitality of Prof. Hong Sun when he visited the University of California at Berkeley and useful discussion with Prof. G. Q. Gu.

REFERENCES

- [1] For a review, see J. Gimsa and D. Wachner, *Biophys. J.* **77**, 1316 (1999).
- [2] J. Gimsa, *Ann. NY Acad. Sci.* **873**, 287 (1999).
- [3] K. Asami, T. Hanai and N. Koizumi, *Jpn. J. Appl. Phys.* **19**, 359 (1980).
- [4] G. Fuhr, J. Gimsa and R. Glaser, *Stud. Biophys.* **108**, 149 (1985).
- [5] J. Gimsa, P. Marszalek, U. Lowe and T. Y. Tsong, *Biophys. J.* **73**, 3309 (1991).
- [6] G. De Gasperis, X.-B. Wang, J. Yang, F. F. Becker and P. R. C. Gascoyne, *Meas. Sci. Technol.* **9**, 518 (1998).
- [7] D. J. Bergman, *Phys. Rep.* **43**, 379 (1978).
- [8] Jun Lei, Jones T. K. Wan, K. W. Yu and Hong Sun, *Phys. Rev. E* **64**, 012903 (2001).
- [9] K. P. Yuen and K. W. Yu, *J. Phys.: Condens. Matter* **9**, 4669 (1997).
- [10] L. Gao, Jones T. K. Wan, K. W. Yu and Z. Y. Li, *J. Phys.: Condens. Matter* **12**, 6825 (2000).
- [11] J. P. H. Burt, K. L. Chan, D. Dawson, A. Parton and R. Pethig, *Ann. Biol. Clin.* **54**, 253 (1996); see also <http://www.ibmm.informatics.bangor.ac.uk/pages/science/rot.htm> for the basic science of electrorotation.
- [12] K. W. Yu, Hong Sun and Jones T. K. Wan, *Physica B* **279**, 78 (2000).

FIGURES

FIG. 1. Upper panels: s_1 and f_{c1} plotted against x for different L_z at $z = 2$. Lower panels: s_2 and f_{c2} plotted against x for different L_z at $z = 2$.

FIG. 2. $-\text{Im}(b_z/2 + b_{xy}/2)$ and $-\text{Im}b_z/2$ are plotted against frequency ω for different L_z at $z = 6$, $x = 2$ and $\sigma_2 = 2.9 \times 10^{-5} \text{Sm}^{-1}$.

FIG. 3. s_1 and f_c are plotted versus x for different z as $L_z = 1/3$ (i.e., spherical shape).

FIG. 4. Curve fitting for $L_z = 1/3$ (i.e., spherical particles).

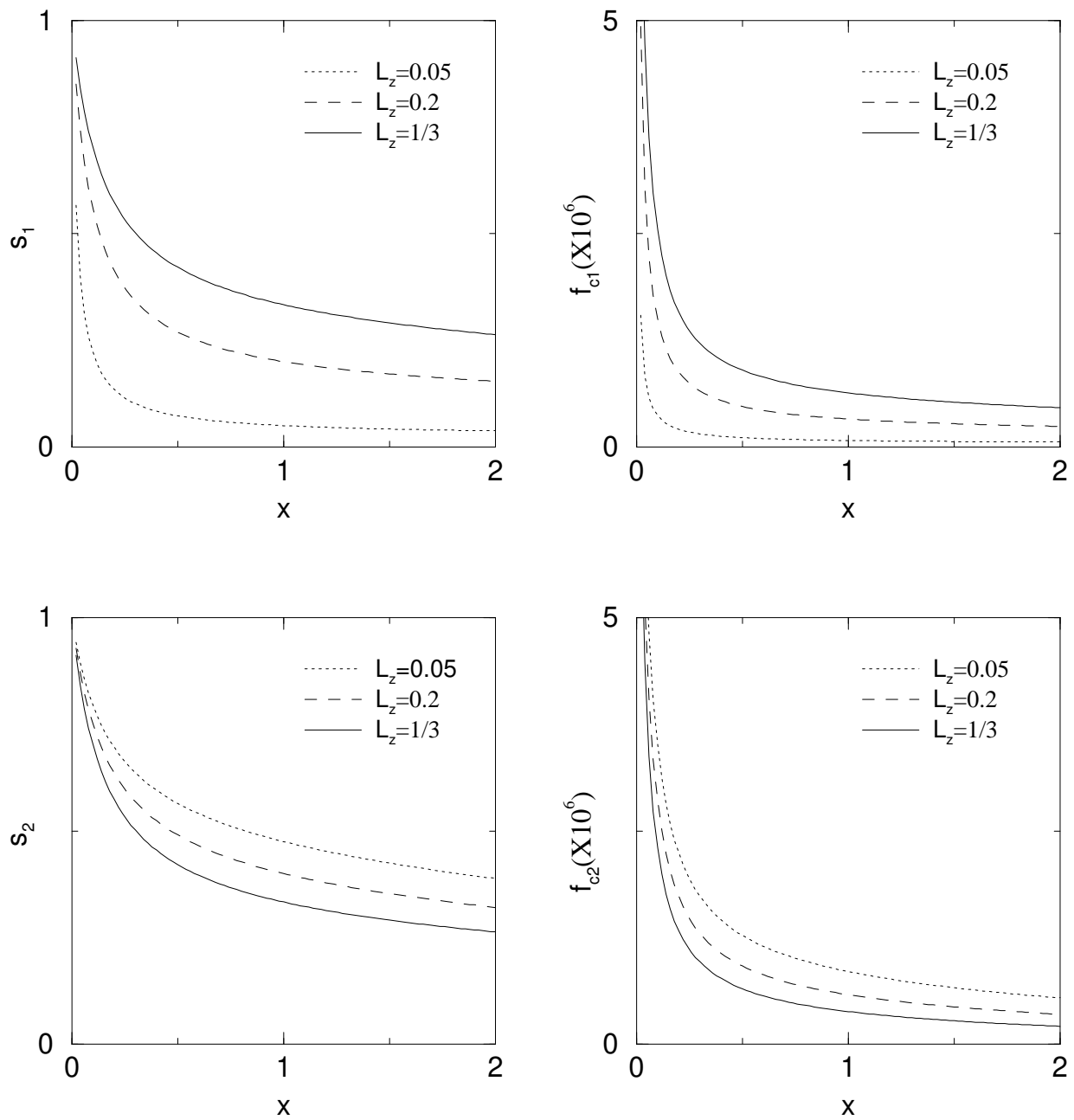


Fig.1

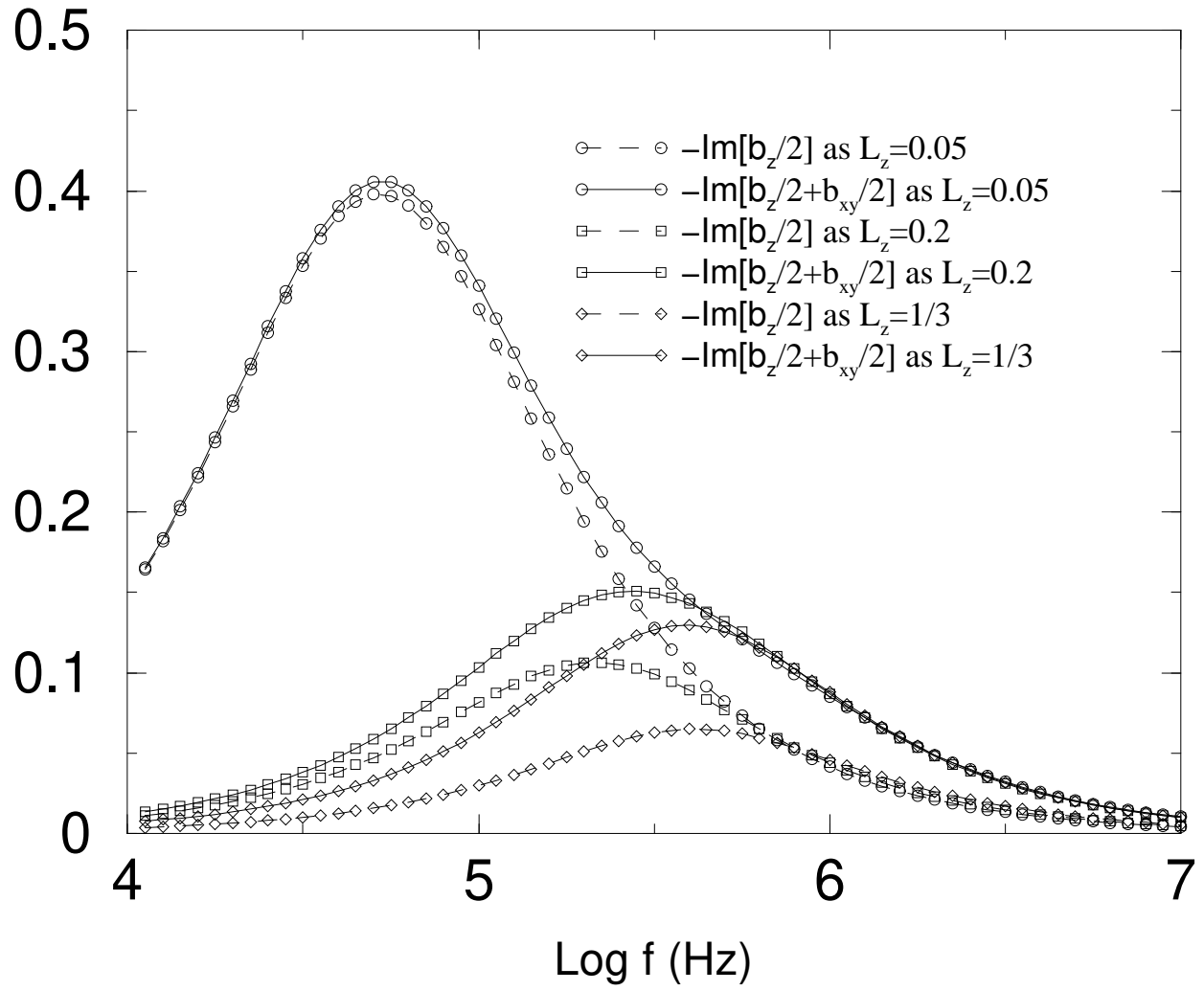


Fig.2

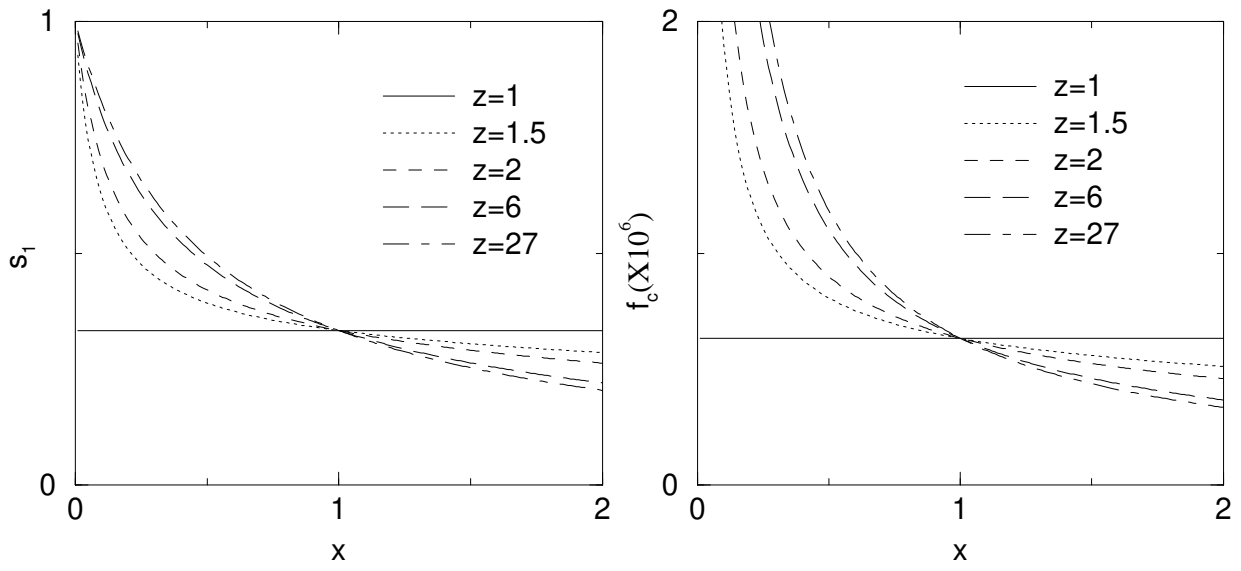


Fig.3

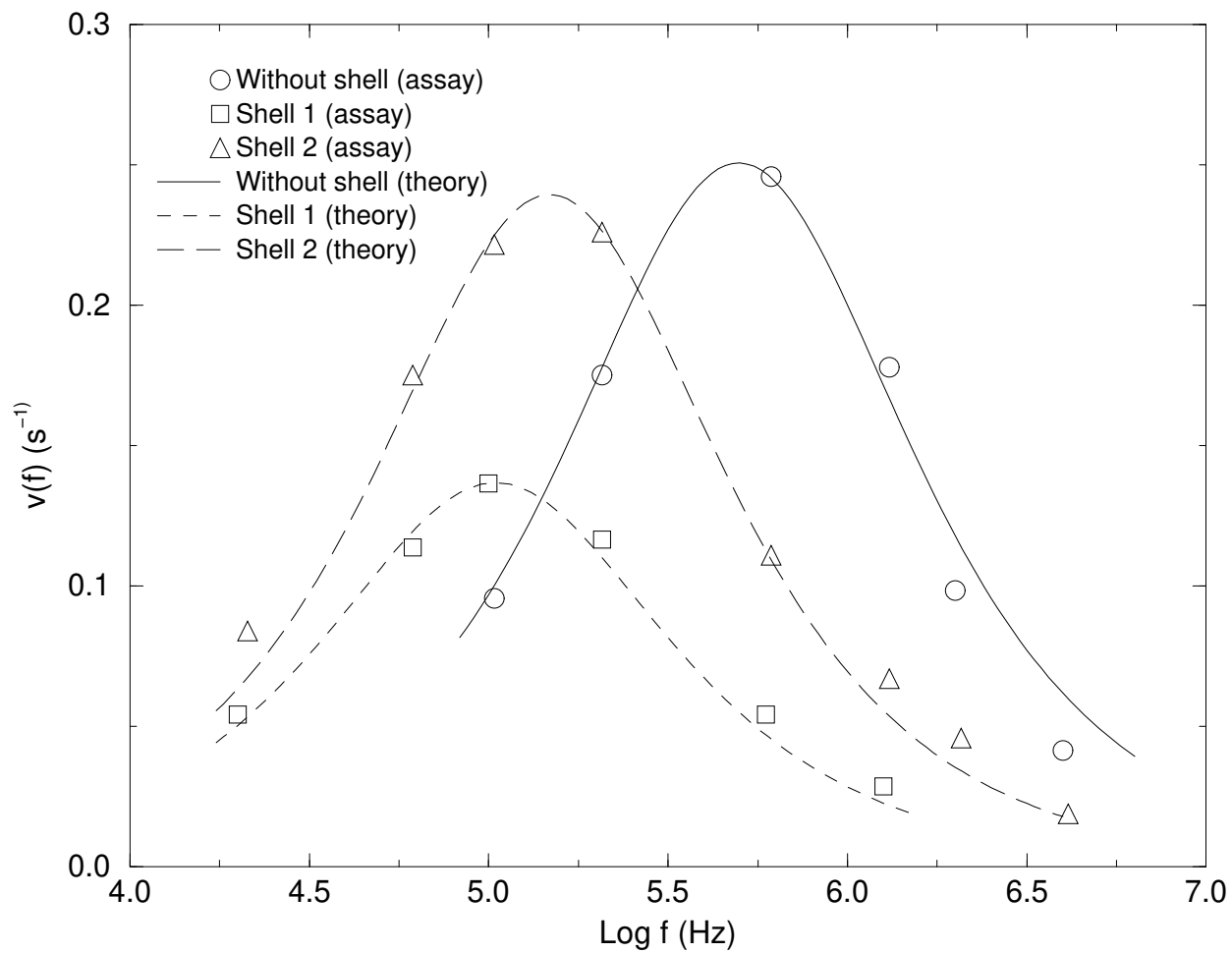


Fig.4